A Hybrid Signalling Scheme for Cellular Mobile Networks over Flat Fading

Hassan A. Abou Saleh and Steven D. Blostein
Dept. of Electrical and Computer Eng.
Queen's University, Kingston, K7L 3N6 Canada
hassan.abousaleh@gmail.com steven.blostein@queensu.ca

***Abstract*—Although recent studies have shown the potential benefits of base station (BS) cooperation technology, existing schemes rely on the assumptions of (i) perfect backbone links between the central network controller (CNC) and the base stations (BSs), and (ii) mobile stations (MSs) at the cell edges. The contribution of this paper is twofold. The authors first relax the aforementioned assumptions and present an in-depth investigation of their impact on the performance of conventional and BS cooperation transmission techniques. A hybrid signalling algorithm for cellular multiple-input multiple-output (MIMO) networks that performs well under such non-ideal scenarios is then presented. The proposed algorithm outperforms the joint transmitter minimum mean squared error (JT-MMSE) method at low to moderate signal-to-noise ratios (SNRs). It is also shown to be more robust to imperfect channel estimates than the JT-MMSE method.**

I. INTRODUCTION

Spatial multiplexing cooperative base station (BS) systems, in which neighboring base stations (BSs) are connected to form a virtual multiple-input multiple-output (MIMO) array, have been recently shown to significantly increase the spectrum efficiency of the downlink cellular MIMO network [1]. The main idea is to let BSs collaboratively and simultaneously transmit data streams to multiple mobile stations (MSs). If each BS has perfect knowledge of all data and channel state information at transmitters (CSIT) (i.e., perfect cooperation), then significant capacity and spatial diversity gains can be obtained by appropriately designing the transmit precoding matrices. Under perfect cooperation, the multi-cell MIMO downlink can be modeled as the classical MIMO broadcast channel (MIMO-BC) with per-base power constraints. The optimal dirty-paper coding (DPC), with a pooled power constraint can then be used across BSs in a straightforward manner [2].

The concept of BS coordination was first studied in [3] in the context of single antenna transmitters and receivers in each cell. In [3], the authors present a relatively simple application of DPC called linear pre-processing dirty paper (LP-DP). The latter is shown to be asymptotically optimal at high signal-to-noise ratios (SNRs). The case of BS cooperation in the multi-cell MIMO downlink is treated in [4]. The maximum achievable common rate in downlink multi-cell coordinated networks, with zero forcing (ZF) and DPC is studied in [5], [6].

In all the above references, perfect and global CSIT is assumed. In practice, there are limitations in terms of global and perfect CSIT and capacity of all the links. The impact of limited capacity backbone links has been recently treated in [7]. Precoding strategies that exploit only local CSIT have been also recently addressed in [8]. Another important issues are (i) the impact of channel estimation errors and MSs locations on the performance of conventional and BS cooperation techniques, and (ii) efficient design strategies that perform well under such non-ideal scenarios. To the best of the authors' knowledge, these issues have not been explicitly addressed previously.

The above observations motivate investigation of the influence of imperfect channel knowledge (i.e., MS-BS or equivalently CNC-BS links) and MSs locations on the aggregate sum rate capacity of both conventional single cell signalling and BS cooperation schemes. We further propose a hybrid signalling algorithm for cellular MIMO networks that outperforms the joint transmitter, in terms of mean squared error (JT-MMSE), and conventional methods at low-to-moderate and high SNRs, respectively. Moreover, the proposed algorithm is shown to be more robust to imperfect channel estimates than the JT-MMSE approach.

The rest of the paper is organized as follows. In Section II, we set up the system model and present the theory. An in-depth investigation into the influence of imperfect channel knowledge and MSs locations is presented in Section III. The hybrid signalling algorithm is also described in Section III.

II. SYSTEM MODEL AND THEORY

We consider the downlink of a TDMA/FDMA cellular network that consists of hexagonal cell patterns. We denote by r the radius of each cell which is assumed to be identical for all cells. There are B co-channel adjacent BSs connected to a CNC via high speed Ethernet backbone links, and K co-channel MSs each equipped with N_t and N_r antennas, respectively. Each cell is loaded with at most one MS for each orthogonal dimension, and partitioned into three 120° sectors. MSs are uniformly distributed in the three interfering sectors as depicted in Fig. 1 for $B = 3$.

H. Abou Saleh was supported in part by a continuing Natural Sciences and Engineering Research Council of Canada (NSERC) postgraduate scholarship (PGS D3). This research was supported by the Natural Sciences and Engineering Research Council of Canada Discovery Grant 41731.

978-1-4244-5711-3/10/$26.00 ©2010 IEEE

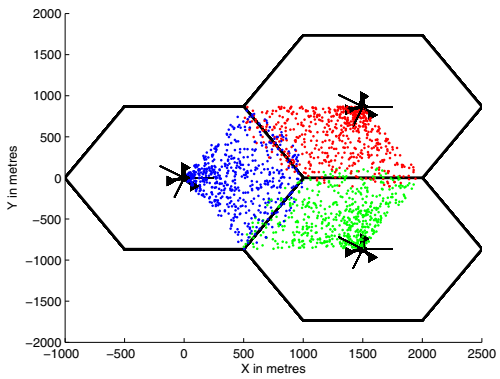

Fig. 1. Snapshot showing distribution of users in network over many trials.

Let $\mathbf{x}_j$, of size $N_t \times 1$, be the signal transmit vector for base station BS$_j$ with $1 \leq j \leq B$. The mobile radio propagation channel model is assumed to be narrowband with frequency-flat block fading such that it remains constant within a given frame of data but varies independently from frame to frame (i.e., low mobility environment). The baseband equivalent of the N_t-dimensional transmitted signal vector, once observed at MS$_k$, can be expressed as

$$\mathbf{y}_k = \sum_{j=1}^{B} c_{jk}\mathbf{H}_{jk}\mathbf{x}_j + \mathbf{n}_k, \quad \text{for } 1 \leq k \leq K, \tag{1}$$

where $\mathbf{y}_k$ is the $N_r \times 1$ corresponding received vector at MS$_k$, $\mathbf{H}_{jk}$ is the $N_r \times N_t$ channel impulse response matrix of the link from BS$_j$ to MS$_k$, which is assumed to experience long term fading $c_{jk} = \sqrt{\alpha\left(\frac{1}{d_{jk}^{\gamma}}\right)}$ with α a propagation constant, d_{jk} the distance between BS$_j$ and MS$_k$, and γ the path loss exponent. The $N_r \times 1$ noise vector $\mathbf{n}_k$ is assumed to be white and complex Gaussian with covariance matrix $N_0\mathbf{I}_{N_r}$, where $\mathbf{I}_{N_r}$ is the identity matrix of dimension N_r. In the following, we introduce both conventional and BS cooperation transmission techniques.

A. BS Cooperation: Joint Precoding

Here, each BS has essentially complete knowledge of all data symbols intended for all MSs and CSI (i.e., all $\mathbf{H}_{jk}$ in (1)). This will enable joint transmitter precoding.

The signal transmitted by BS$_j$ can then be written as

$$\mathbf{x}_j = \sum_{k=1}^{K} \mathbf{W}_{jk}\mathbf{s}_k, \quad \text{for } 1 \leq j \leq B, \tag{2}$$

where $\mathbf{W}_{jk}$ is the $N_t \times N_r$ transmit linear precoding matrix of MS$_k$ from BS$_j$ and $\mathbf{s}_k$ is the data symbol vector intended for MS$_k$. To maximize the per-user information rate, we use a Gaussian codebook with normalized transmit power for the data symbol vector intended for MS$_k$ [4], i.e., $\mathbf{s}_k \in \mathcal{CN}(\mathbf{0}, \mathbf{I}_{N_r})$. BS$_j$ is subject to a transmit power constraint of P_j, i.e., $\mathbb{E}\left[\|\mathbf{x}_j\|^2\right] = \sum_{k=1}^{K} \text{tr}\left(\mathbf{W}_{jk}\mathbf{W}_{jk}^H\right) \leq P_j$, where $\mathbb{E}[\cdot]$ stands for expectation, tr$(\cdot)$ denotes trace, and $(\cdot)^H$ refers to Hermitian transpose.

Substituting (2) in (1), after some manipulation we get

$$\begin{aligned}\mathbf{y}_k &= \sum_{j=1}^{B} c_{jk}\mathbf{H}_{jk}\mathbf{W}_{jk}\mathbf{s}_k + \sum_{\substack{\bar{k}=1 \\ \bar{k}\neq k}}^{K}\sum_{j=1}^{B} c_{jk}\mathbf{H}_{jk}\mathbf{W}_{j\bar{k}}\mathbf{s}_{\bar{k}} + \mathbf{n}_k \\ &= \mathbf{H}_k\mathbf{W}_k\mathbf{s}_k + \sum_{\substack{\bar{k}=1 \\ \bar{k}\neq k}}^{K} \mathbf{H}_k\mathbf{W}_{\bar{k}}\mathbf{s}_{\bar{k}} + \mathbf{n}_k, \quad \text{for } 1 \leq k \leq K,\end{aligned} \tag{3}$$

where the $N_r \times BN_t$ aggregate propagation channel matrix $\mathbf{H}_k = [c_{1k}\mathbf{H}_{1k}, c_{2k}\mathbf{H}_{2k}, \ldots, c_{Bk}\mathbf{H}_{Bk}]$, the $BN_t \times N_r$ matrix $\mathbf{W}_k = \left[\mathbf{W}_{1k}^H, \mathbf{W}_{2k}^H, \ldots, \mathbf{W}_{Bk}^H\right]^H$, and $\bar{k}$ denotes the value not being k. The aim of BS cooperation is to properly design the BS precoding matrices $\{\mathbf{W}_k,\ 1 \leq k \leq K\}$ to eliminate the interfering signals in (3). The optimal DPC and LP-DP algorithms are very complex and serve only as theoretical upper bounds. From this fact stems the necessity to design more practical schemes with per-base power constraints [4], [9]:

1) *Joint transmitter ZF (JT-ZF)*

$$\mathbf{W}_T = \mathbf{H}_T^H\left(\mathbf{H}_T\mathbf{H}_T^H\right)^{-1}, \tag{4}$$

where the $BN_t \times KN_r$ $\mathbf{W}_T = [\mathbf{W}_1, \ldots, \mathbf{W}_K]$, and $\mathbf{H}_T = \left[\mathbf{H}_1^H, \ldots, \mathbf{H}_K^H\right]^H$ is of size $KN_r \times BN_t$. Note that $\mathbf{W}_k$ and $\mathbf{H}_k$ are defined in (3).

2) *Joint transmitter MMSE (JT-MMSE)*

$$\mathbf{W}_T = \mathbf{H}_T^H\left(\mathbf{H}_T\mathbf{H}_T^H + \frac{N_0}{P_T}\mathbf{I}\right)^{-1}, \tag{5}$$

where $P_T = \sum_{j=1}^{B} P_j$.

3) *Joint transmitter null-space decomposition (JT-decomp)*

$$\mathbf{W}_k = \mathbf{V}_{\bar{k}}\mathbf{V}'_k, \tag{6}$$

where $\mathbf{V}_{\bar{k}}$ consists of the right singular vectors corresponding to the null space of $(\mathbf{H}_T)_{\bar{k}} = \left[\mathbf{H}_1^H, \ldots, \mathbf{H}_{k-1}^H, \mathbf{H}_{k+1}^H, \ldots, \mathbf{H}_K^H\right]^H$, and $\mathbf{V}'_k$ contains the first N_r right singular vectors of the virtual channel $\mathbf{H}'_k = \mathbf{H}_k\mathbf{V}_{\bar{k}}$. The JT-decomp method is more complex than each of JT-ZF and JT-MMSE methods [4].

Based on (3), the instantaneous transmission rate at the MS$_k$ with the above suboptimal linear transmission algorithms is

$$R_k^{\text{linear-coop}} = \log_2 \det\left[\mathbf{I}_{N_r} + \mathbf{\Phi}_k^{-1}\mathbf{H}_k\mathbf{W}_k\mathbf{W}_k^H\mathbf{H}_k^H\right], \tag{7}$$

where $\mathbf{\Phi}_k = (N_0\mathbf{I}_{N_r} + \mathbf{H}_k(\sum_{\substack{\bar{k}=1 \\ \bar{k}\neq k}}^{K} \mathbf{W}_{\bar{k}}\mathbf{W}_{\bar{k}}^H)\mathbf{H}_k^H)$, and det$(\cdot)$ stands for determinant.

B. Non-Cooperation: Single Cell Precoding

Here BSs do not share CSI and data symbols, and as a result, no joint precoding is done at the transmitters. For ease of presentation and due to the fact that communication is restricted to only one active pair in each cell, we let BS$_k$

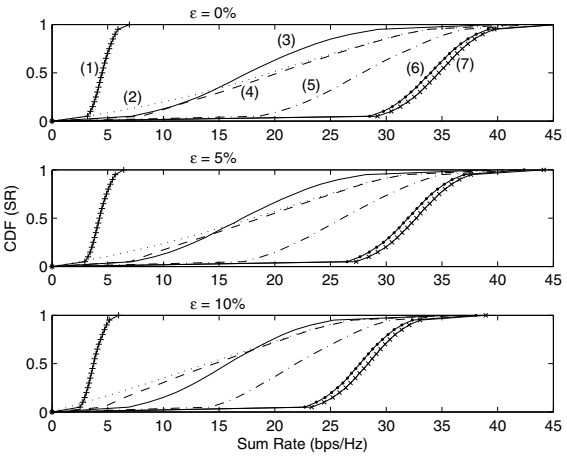

Fig. 2. CDF of the sum rate capacity at SNR = 20 dB of a $[(3,2),(3,2)]$ system using conventional and BS cooperation schemes with various CSI error settings. (1) TDMA (Solid line with plus-sign markers); (2) JT-ZF (Dotted line); (3) conv_{LB} (Solid line); (4) JT-MMSE (Dashed line); (5) JT-decomp (Dash-dot line); (6) conv_{UB} (Solid line with point markers); (7) LP-DP (Solid line with cross markers).

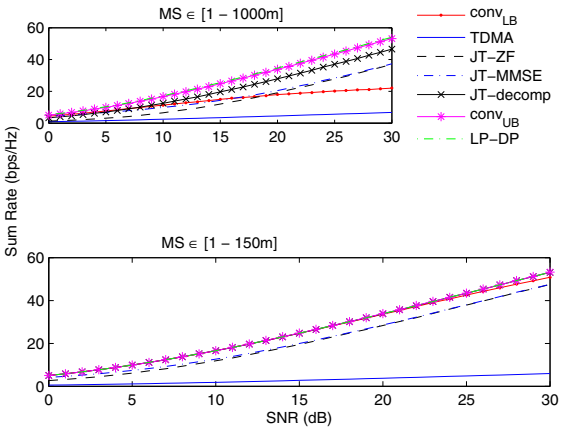

Fig. 3. Average sum rate of a $[(3,2),(3,2)]$ system using conventional and cooperation schemes with various MSs position settings.

(instead of BS_j) denote the serving BS of MS_k. The signal transmitted by BS_k to MS_k can then be written as

$$\mathbf{x}_k = \mathbf{W}_{kk}\mathbf{s}_k, \quad \text{for } 1 \le k \le K, \tag{8}$$

where $\mathbf{W}_{kk}$ is the precoding matrix for MS_k (see Eq. (2)). A power constraint of $\mathbb{E}\left[\|\mathbf{x}_k\|^2\right] = \text{tr}\left(\mathbf{W}_{kk}\mathbf{W}_{kk}^H\right) \le P_k$ holds at each BS. Based on (8), Eq. (1) can be rewritten as

$$\mathbf{y}_k = c_{kk}\mathbf{H}_{kk}\mathbf{W}_{kk}\mathbf{s}_k + \sum_{\substack{\bar{k}=1 \\ \bar{k}\neq k}}^{K} c_{\bar{k}k}\mathbf{H}_{\bar{k}k}\mathbf{W}_{\bar{k}\bar{k}}\mathbf{s}_{\bar{k}} + \mathbf{n}_k, \tag{9}$$

with $1 \le k \le K$, $\mathbf{H}_{kk}$ of size $N_r \times N_t$ denote the baseband channel between BS_k and MS_k. $\mathbf{W}_{kk}$ can be determined by eigen-beamfroming and water-filling power allocation on each data stream to each MS [10]. Assuming single user detection, a lower bound for the instantaneous transmission rate at MS_k is

$$R_k^{\text{conv-LB}} = \log_2 \det\left[\mathbf{I}_{N_r} + \frac{c_{kk}^2}{\Phi_k}\mathbf{H}_{kk}\mathbf{W}_{kk}\mathbf{W}_{kk}^H\mathbf{H}_{kk}^H\right], \tag{10}$$

where $\Phi_k = N_0 + \sum_{\substack{\bar{k}=1 \\ \bar{k}\neq k}}^{K} c_{\bar{k}k}^2 P_{\bar{k}}$. The instantaneous interference-free (i.e., upper bound) transmission rate is

$$R_k^{\text{conv-UB}} = \log_2 \det\left[\mathbf{I}_{N_r} + \frac{c_{kk}^2}{N_0}\mathbf{H}_{kk}\mathbf{W}_{kk}\mathbf{W}_{kk}^H\mathbf{H}_{kk}^H\right]. \tag{11}$$

III. Results and Hybrid Signalling Algorithm

In Section II, we have introduced conventional and BS cooperation techniques. The effects of imperfect channel estimation and MSs positions on their performance are now investigated. Performance results are reported in terms of average sum rate capacity versus SNR in dB. In the following, a system with B BSs (each with N_t transmit antennas) and K MSs (each with N_r receive antennas) is referred to as an $[(B,N_t),(K,N_r)]$ system. Henceforth, we consider: (i) $[(3,2),(3,2)]$ system; (ii) cell radius is set to $r = 1000$m; (iii) path loss coefficient is $\gamma = 3$; Without loss of generality, the channel path loss values are normalized with respect to the largest in-cell path loss value [11]; (iv) Rayleigh fading model; (v) all BSs have power of unity; (vi) the power allocation algorithms in [4] are adopted; (vii) channel estimation errors are modeled as zero-mean complex Gaussian random variables with covariance matrix $\left(\frac{\epsilon^2}{1-\epsilon^2}\right)\mathbf{I}_{N_r}$, where $\epsilon \in [0,1]$ is the mean square error of the channel estimation [12], [13]; and (viii) the propagation constant, $\alpha = 1.35 \times 10^7$ [4], [14].

A. Impact of Channel Estimation Errors

The influence of channel estimation errors on the system sum rate capacity with conventional and BS cooperation algorithms is exhibited in Fig. 2. We plot the cumulative distribution function (CDF) of sum rate capacity with SNR = 20 dB. As theoretical reference points, LP-DP and the upper bound (11) are also evaluated. To focus on the impact of channel estimation errors, we assume that MSs are uniformly distributed inside the three interfering sectors. Three CSI error settings are considered: (i) $\epsilon = 0$ (error free case); (ii) $\epsilon = 0.05$; and (iii) $\epsilon = 0.1$. In the following, we consider 10% outage capacity. With $\epsilon = 0\%$, 9.4 bits/s/Hz can be transmitted with both conventional and JT-MMSE, whereas JT-ZF achieves only 5.8 bits/s/Hz. For $\epsilon = 10\%$, 8.7 bits/s/Hz can be transmitted with the conventional scheme, whereas 5.6 and 3 bits/s/Hz can be transmitted with JT-MMSE and JT-ZF, respectively. These observations verify in part the robustness of the conventional scheme to channel estimation errors. This is because, in contrast to the conventional technique, erroneous CSI in the case of linear BS cooperation transmissions results in significant mutual interference. Thus, linear BS cooperation techniques are expected to be sensitive to channel estimation errors.

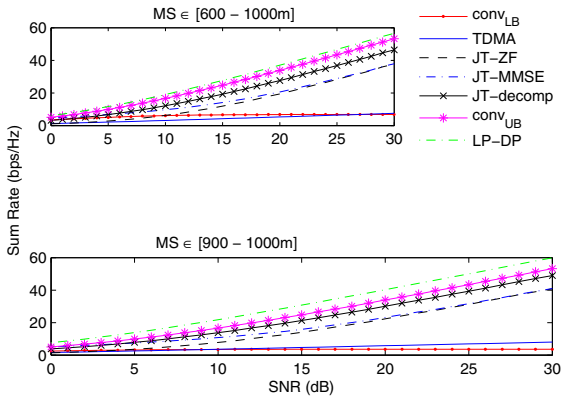

Fig. 4. Average sum rate of a $[(3,2),(3,2)]$ system using conventional and BS cooperation techniques with various cell edge MSs position settings.

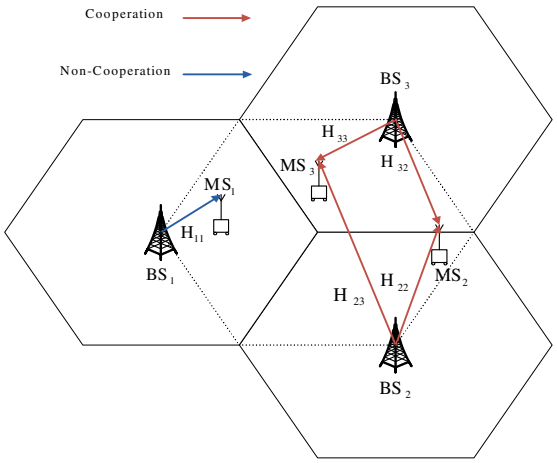

Fig. 5. Simple scenario of a $[(3,2),(3,2)]$ system employing hybrid transmission (multi-mode) technique.

B. Impact of Position of Mobiles

To focus on the impact of MSs positions, perfect CSIT is assumed. Figs. 3 and 4 illustrate the influence of MSs positions on the average sum rate system capacity with conventional and BS cooperation methods. From Fig. 3 and from our other simulations (not included here), we observe that both conventional and cooperation schemes show gradual improvement as the distance between MSs and their serving BSs decreases. However, we stress that the conventional scheme improves faster than the others and achieves a significant gain. For instance, at SNR $= 30$ dB the gain is about 25 bits/s/Hz for conventional signalling, whereas it is about 8 bits/s/Hz for each of JT-decomp, JT-MMSE, and JT-ZF. From Fig. 4, it can be observed that as MSs are located closer to cell edges, BS cooperation techniques perform better than the conventional signalling method. At SNR $= 30$ dB, the gap in gain is about 38 bits/s/Hz in favor of both JT-MMSE and JT-ZF. To sum up, we note the following: (i) it is wiser to adopt BS cooperation techniques when MSs are at cell edge; and (ii) linear BS cooperation techniques achieve their best performance when MSs are close to their serving BSs. This agrees with intuition since, in this case, a dominant eigenmode for each user is present and also interference is reduced (see Eqs. (3) and (7)). From an information-theoretic point of view, the sum rate capacity is then higher.

C. Hybrid Signalling Algorithm

We now propose a hybrid signalling algorithm that switches between three different transmission modes: (i) full non-cooperation mode (i.e., conventional), (ii) full linear BS cooperation mode such as JT-MMSE and JT-ZF methods, and (iii) multi-mode (i.e., cooperation and non-cooperation modes simultaneously) based on received signal strength measurements and MSs position. All the aforementioned observations lead to the following algorithm.

1) *IF* all MSs are randomly located in a limited cell edge area, i.e., the distance between each MS and its corresponding in-cell BS is $> 0.6\,r$ with r the cell radius
   $\rightarrow$ linear BS cooperation techniques are employed for all MSs.
2) *ELSE*
   a) indices$^{\text{conv.}} = [\,]$; indices$^{\text{coop.}} = [\,]$.
   b) *LOOP* over $k \in \{1, 2, \ldots, K\}$
      i) Compute

$$|\mathbf{H}_{\bar{k}}| = \big[\, \|c_{1k}\mathbf{H}_{1k}\|, \ldots, \|c_{k-1,k}\mathbf{H}_{k-1,k}\|, \|c_{k+1,k}\mathbf{H}_{k+1,k}\|, \ldots, \|c_{Bk}\mathbf{H}_{Bk}\| \,\big].$$

      The vector $|\mathbf{H}_{\bar{k}}|$ consists of entries that represent magnitude of the channels between the BSs of neighboring cells and MS$_k$.
      ii) *IF* the difference between $\|c_{kk}\mathbf{H}_{kk}\|$ and the sum of the entries of $|\mathbf{H}_{\bar{k}}|$ is high (e.g., $>$ threshold Ξ), in this case the signal from the in-cell BS (i.e., $c_{kk}\mathbf{H}_{kk}$) does completely dominate the signal from the BSs of neighbouring cells
      $\rightarrow$ the conventional approach is adopted for MS$_k$, i.e., indices$^{\text{conv.}} = [\text{indices}^{\text{conv.}}\ k]$.
      iii) *ELSE* $c_{kk}\mathbf{H}_{kk}$ does not completely dominate the signal from the BSs of neighbouring cells
      $\rightarrow$ MS$_k$ should operate in cooperation mode, i.e., indices$^{\text{coop.}} = [\text{indices}^{\text{coop.}}\ k]$.
      iv) *ENDIF*
   c) *ENDLOOP*
   d) *IF* length (indices$^{\text{coop.}}$) $== 1$
      $\rightarrow$ reassign the corresponding MS$_k$ to the set of MSs operating in non-cooperative mode of transmissions.
   e) *ENDIF*.
3) *ENDIF*.

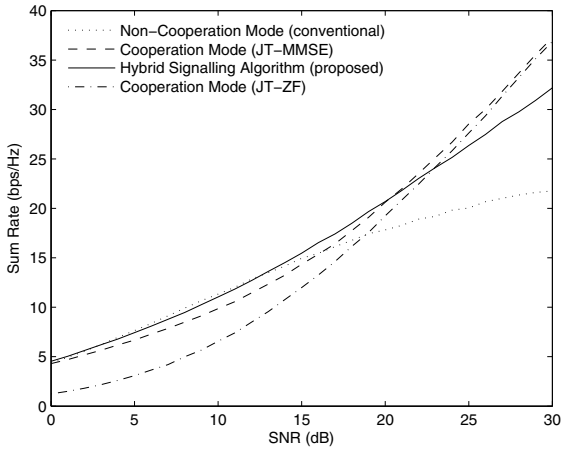

Fig. 6. Average sum rate of a $[(3,2),(3,2)]$ system using hybrid, JT-MMSE, JT-ZF, and conventional transmission techniques. $\Xi = 1.65$, perfect CSI, and MSs $\in$ [1-1000m].

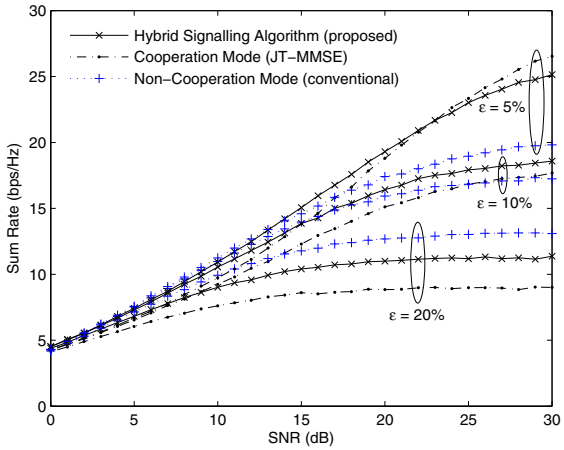

Fig. 8. Average sum rate of a $[(3,2),(3,2)]$ system using hybrid, JT-MMSE, and conventional transmission techniques with various CSI error settings. $\Xi = 1.65$ and MSs $\in$ [1-1000m].

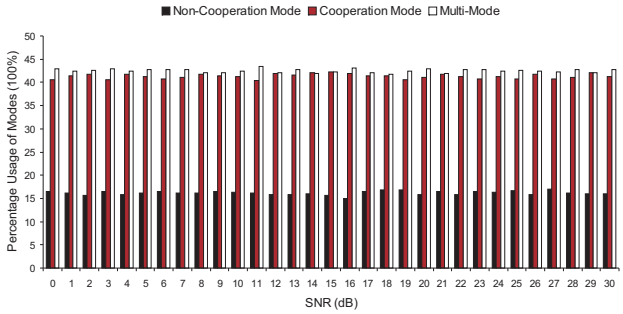

Fig. 7. Usage rate of modes for a $[(3,2),(3,2)]$ system employing hybrid signalling transmission. $\Xi = 1.65$, perfect CSI, and MSs $\in$ [1-1000m].

We stress that both conventional and BS cooperation techniques are not optimal in any scenarios. The hybrid algorihtm builds on this fact to provide different modes of transmission according to the considered scenario. Positioning and signal strength measurements can be realized by GPS or wired backbone which are already available in CDMA2000 and IS-95 cellular networks [11], [15].

A possible simple scenario with hybrid signalling transmission is illustrated in Fig. 5. Notice that MS_1 is operating in non-cooperation mode, whereas MS_2 and MS_3 are operating in cooperation modes. See Appendix for expressions of the received signals, observed at each MS, in this scenario. An interesting point for future work includes efficient joint design of the weight matrices to minimize interference. For instance, the weight matrices of the non-cooperation mode can be designed to maximize the so-called signal to generated inteference plus noise ratio (SGINR) [16].

The performance of the hybrid signalling algorithm is detailed in Fig. 6. For comparison, JT-MMSE, JT-ZF, and conventional techniques are also evaluated. We note the following: (i) the hybrid and the conventional algorithms exhibit similar performance in $[0-13]$ dB. At SNR $= 11$ dB, 11.85 bits/s/Hz can be transmitted with conventional and hybrid algorithms, whereas the JT-MMSE algorithm achieves only 10.5 bits/s/Hz; (ii) in $[0-21]$ and $[0-23]$ dB, the hybrid algorithm outperforms the JT-MMSE and the JT-ZF methods, respectively; and (iii) with SNR > 23 dB, the hybrid algorithm is much closer to each of JT-ZF and JT-MMSE methods than the conventional approach is. At SNR $= 30$ dB, 37 bits/s/Hz can be transmitted with JT-MMSE, whereas 32.2 and 21.8 bits/s/Hz can be transmitted with hybrid and conventional approaches, respectively. Keep in mind that in a realistic cellular environment the edge SNR is typically around 18 dB [17].

Fig. 7 illustrates the usage rate of each mode for a $[(3,2),(3,2)]$ system employing hybrid transmission technique. It can be observed that the usage rate of multi and full cooperation modes are similar with about 43% and 40% usage over all SNRs, respectively, whereas the rate of usage of the full non-cooperation mode is about 17% over all SNRs.

Fig. 8 shows the impact of channel estimation errors on the sum rate capacity of a $[(3,2),(3,2)]$ system using conventional, JT-MMSE, and hybrid signalling approaches with various CSI error settings. Notice that (i) the conventional approach is more robust to imperfect channel knowledge than each of JT-MMSE and hybrid methods. At SNR $= 30$ dB and with $\epsilon = 5\%$, the capacity loss is about 10 bits/s/Hz with JT-MMSE algorithm, whereas it is 7 and 2 bits/s/Hz with hybrid and conventional algorithms, respectively; (ii) the hybrid signalling algorithm is more robust against channel estimation errors than the JT-MMSE method. This is mainly due to the decrease in the usage of JT-MMSE mode when using hybrid transmission. Keep in mind that the JT-MMSE method is very sensitive to imperfect channel estimates since it requires the computation of a matrix inverse to precode. In other words, this is mainly due to the presence of non-

cooperation and multi modes (see Fig. 7). (iii) an error floor exists when $\epsilon > 5\%$ which increases as ϵ increases; and (iv) with $\epsilon = 10\%$, the hybrid algorithm outperforms the JT-MMSE and the conventional methods, where the capacity of the hybrid algorithm hits an error floor of about 18.6 bits/s/Hz.

IV. SUMMARY AND CONCLUSION

We have investigated the behavior of cellular networks employing both conventional and BS cooperation techniques, under non-ideal scenarios. The most important results and insights are the following: (i) we have shown that BS cooperation techniques achieve significant gain, compared to the conventional approach, when MSs are limited to cell edge area. But the conventional scheme performs best when the signal from one BS dominates the signal from BSs of neighboring cells; (ii) we have proposed a hybrid signalling algorithm for cellular mobile networks that performs well under such non-ideal scenarios; and (iii) we have shown that the conventional method is more robust against channel estimation errors than each of JT-MMSE, JT-ZF, and hybrid methods. We have also shown that, in turn, the hybrid algorithm is more robust to imperfect channel estimates than the JT-MMSE algorithm. This paper thus provides useful insights into design of transmission techniques for cellular networks under non-ideal scenarios. Future work will include joint efficient design of weight matrices based on weighted channel gain estimates.

APPENDIX

We now give the expressions of the baseband received signals, observed at MSs, when hybrid transmission (multi-mode) is used as depicted in Fig. 5.

The sampled received baseband signal at MS_1 is given by

$$\mathbf{y}_1 = c_{11}\mathbf{H}_{11}\mathbf{x}_1 + (\mathbf{n}_1 + c_{31}\mathbf{H}_{31}\mathbf{x}_3 + c_{21}\mathbf{H}_{21}\mathbf{x}_2), \quad (12)$$

where $(c_{31}\mathbf{H}_{31}\mathbf{x}_3 + c_{21}\mathbf{H}_{21}\mathbf{x}_2)$ is the interference signal from BS_2 and BS_3, $\mathbf{x}_1 = \mathbf{W}_{11}\mathbf{s}_1$, $\mathbf{x}_2 = (\mathbf{W}_{22}\mathbf{s}_2 + \mathbf{W}_{23}\mathbf{s}_3)$, and $\mathbf{x}_3 = (\mathbf{W}_{33}\mathbf{s}_3 + \mathbf{W}_{32}\mathbf{s}_2)$.

The sampled received baseband signal at MS_2 can be written as

$$\begin{aligned}\mathbf{y}_2 &= [c_{22}\mathbf{H}_{22},\ c_{32}\mathbf{H}_{32}]\left[\mathbf{W}_{22}^H,\ \mathbf{W}_{32}^H\right]^H\mathbf{s}_2 \\ &+ (\mathbf{n}_2 + [c_{22}\mathbf{H}_{22},\ c_{32}\mathbf{H}_{32}]\left[\mathbf{W}_{23}^H,\ \mathbf{W}_{33}^H\right]^H\mathbf{s}_3 \\ &+ c_{12}\mathbf{H}_{12}\mathbf{W}_{11}\mathbf{s}_1), \end{aligned} \quad (13)$$

with $c_{12}\mathbf{H}_{12}\mathbf{W}_{11}\mathbf{s}_1$ the interference signal from BS_1.

The sampled received baseband signal at MS_3 can be expressed as

$$\begin{aligned}\mathbf{y}_3 &= [c_{33}\mathbf{H}_{33},\ c_{23}\mathbf{H}_{23}]\left[\mathbf{W}_{33}^H,\ \mathbf{W}_{23}^H\right]^H\mathbf{s}_3 \\ &+ \mathbf{n}_3 + [c_{33}\mathbf{H}_{33},\ c_{23}\mathbf{H}_{23}]\left[\mathbf{W}_{32}^H, \mathbf{W}_{22}^H\right]^H\mathbf{s}_2 \\ &+ c_{13}\mathbf{H}_{13}\mathbf{W}_{11}\mathbf{s}_1), \end{aligned} \quad (14)$$

where $c_{13}\mathbf{H}_{13}\mathbf{W}_{11}\mathbf{s}_1$ is the interference signal from BS_1 observed at MS_3.

REFERENCES

[1] A. F. Molisch, L. Dong, P. V. Orlik, and J. Zhang, "Cooperative base stations in wireless networks," U.S. Patent 11/934 131, Nov., 2007.

[2] E. Biglieri, R. Calderbank, A. Constantinides, A. Goldsmith, A. Paulraj, and H. V. Poor, *MIMO Wireless Communications*. New York, USA: Cambridge University Press, 2007.

[3] S. Shamai and B. M. Zaidel, "Enhancing the cellular downlink capacity via co-processing at the transmitting end," in *Proc. IEEE Vehicular Technology Conference (VTC'01)*, Rhodes, Greece, May 2001, pp. 1745–1749.

[4] H. Zhang and H. Dai, "Cochannel interference mitigation and cooperative processing in downlink multicell multiuser MIMO networks," *EURASIP J. Wireless Commun. and Networking*, vol. 2004, pp. 222–235, Dec. 2004.

[5] G. J. Foschini, K. Karakayali, and R. A. Valenzuela, "Coordinating multiple antenna cellular networks to achieve enormous spectral efficiency," *IEE Proceedings-Communications*, vol. 153, pp. 548–555, Aug. 2006.

[6] M. K. Karakayali, G. J. Foschini, and R. A. Valenzuela, "Network coordination for spectrally efficient communications in cellular systems," *IEEE Wireless Commun. Mag.*, vol. 13, pp. 56–61, Aug. 2006.

[7] O. Somekh, O. Simeone, A. Sanderovich, B. M. Zaidel, and S. Shamai, "On the impact of limited-capacity backhaul and inter-users links in cooperative multicell networks." in *Proc. Conference on Information Sciences and Systems (CISS'08)*, Princeton, NJ, Mar. 2008, pp. 776–780.

[8] E. Bjornson, R. Zakhour, D. Gesbert, and B. Ottersten, "Distributed multicell and multiantenna precoding: Characterization and performance evaluation," in *Proc. IEEE Global Communications Conference (GLOBECOM'09)*, Honolulu, Hawaii, Nov. 2009.

[9] Q. H. Spencer, A. L. Swindlehurst, and M. Haardt, "Zero-forcing methods for downlink spatial multiplexing in multiuser MIMO channels," *IEEE Trans. Signal Process.*, vol. 52, pp. 461–471, Feb. 2004.

[10] S. D. Blostein and H. Leib, "Multiple antenna systems: Their role and impact in future wireless access," *IEEE Commun. Mag.*, vol. 41, pp. 94–101, Jul. 2003.

[11] H. Zhang, N. B. Mehta, A. F. Molisch, J. Zhang, and H. Dai, "Asynchronous interference mitigation in cooperative base station systems," *IEEE Trans. Wireless Commun.*, vol. 7, pp. 155–165, Jan. 2008.

[12] X. Zhang and B. Ottersten, "Performance analysis of V-BLAST structure with channel estimation errors," in *Proc. IEEE Workshop on Signal Processing Advances in Wireless Communications (SPAWC'03)*, Rome, Italy, Jun. 2003, p. 487491.

[13] K. Yu and A. Alexiou, "Impact of channel estimation errors on various spatial-temporal transmission schemes," in *Proc. 16th IST Mobile and Wireless Communications Summit*, Budapest, Hungary, Jul. 2007.

[14] T. S. Rappaport, *Wireless Communications: Principles and Practice*. Upper Saddle River, NJ 07458: Prentice Hall, 2002.

[15] H. Zhang, "MIMO communications systems: Antenna selection and interference mitigations," Ph.D. dissertation, North Carolina State University, Aug. 2006.

[16] B. O. Lee, H. W. Je, O.-S. Shin, and K. B. Lee, "A novel uplink MIMO transmission scheme in a multicell environment," *IEEE Trans. Wireless Commun.*, vol. 8, pp. 4981–4987, Oct. 2009.

[17] M. K. Karakayali, "Network coordination for spectrally efficient communications in wireless networks," Ph.D. dissertation, Rutgers, The State University of New Jersey, Jan. 2007.